SLAC-36
UC-28, Particle Accelerators
and High-Voltage Machines
UC-34, Physics
TID-4500 (37th Ed.)

HIGH REPETITION RATE PULSER FOR BEAM SWITCHING MAGNET

February 1965

by

J. L. Cole and J. J. Muray

Technical Report
Prepared Under
Contract AT(04-3)-400
for the USAEC
San Francisco Operations Office

Printed in USA. Price $1.25. Available from the Office of Technical Services, Department of Commerce, Washington 25, D.C.

TABLE OF CONTENTS

LIST OF FIGURES

ACKNOWLEDGMENTS

The authors are grateful to J. Ballam, R. Mozley, R. Taylor and R. Scholl of the Stanford Linear Accelerator Center for many helpful suggestions, and to B. Hedin of CERN for valuable discussions.

SUMMARY

The electron beam from the Stanford two-mile linear accelerator is analyzed by a high-quality magnetic deflection system in the beam switchyard. The first magnet element in this system is a pulsed switching magnet capable of switching beams of different energies and intensities to either transport system on a pulse-to-pulse basis. This magnet actually consists of five one-meter sections and is powered by pulsed high-voltage supplies (modulators). Each magnet section is excited with two modulators because it must pulse in either polarity in order to switch the beam left or right; the pulse height should be continuously variable to accommodate any beam energy. The magnetic field in these magnets rises sinusoidally 360 times a second and has a peak value of 1700 gauss.

In this paper the optical properties of the pulsed magnet will be discussed briefly. Detailed descriptions of the pulsed magnet modulators, the instrumentation for the magnet, and the test results will be given. The problems connected with high-power switching at high repetition rates will also be discussed.

I. GENERAL

The electron beam from the Stanford two-mile linear accelerator is analyzed by a high quality magnetic deflection system in the beam switchyard. The basic elements of the magnetic transport systems with the calculated beam profiles are shown in Fig. 1. The first magnet element in this system is a pulsed switching magnet capable of switching beams of different energies and intensities to either transport system on a pulse-to-pulse basis, 360 times a second. The beam switching magnet should be capable of being pulsed in either polarity in order to switch the beam left or right; the magnetic field in the magnet should be continuously variable in order to accommodate any beam energy.

Building a pulsed magnet system requires that solutions be found for three major problems which are not common to dc magnets. These problems are the magnet design, the vacuum chamber for the magnet gap, and the pulser design.

The first problem is that of designing a magnet which is capable of being pulsed. A solid iron core magnet is not suitable because of hysteresis losses; therefore, other cores must be considered, such as an air core, a ferrite core, or a laminated iron core.

Because the air core magnet does not have an iron circuit, the number of field lines passing through the useful volume of the gap is small, and the stray magnetic field is very extensive. In this low peak field region the air core magnet is inferior to the ferrite or iron core magnets.

The core material for the magnet may be chosen to be ferrite, which has a conductivity of 10^{-7} times that for metals, thus extending eddy current limitations to much higher frequencies. A typical ferrite core magnet has a saturation flux density of $0.2 - 0.3$ (weber/meter^2), which is larger than the required peak field. The disadvantage of this type of core material is its high cost as compared to other core material choices.

A magnet with a laminated iron core would prevent extensive eddy current losses; in addition, its frequency response is adequate and it is economical. Laminated iron thus appeared to be the best core material for the pulsed magnet, and the magnets were designed using laminated H-type cores with multi-stranded water-cooled coils. Details of the

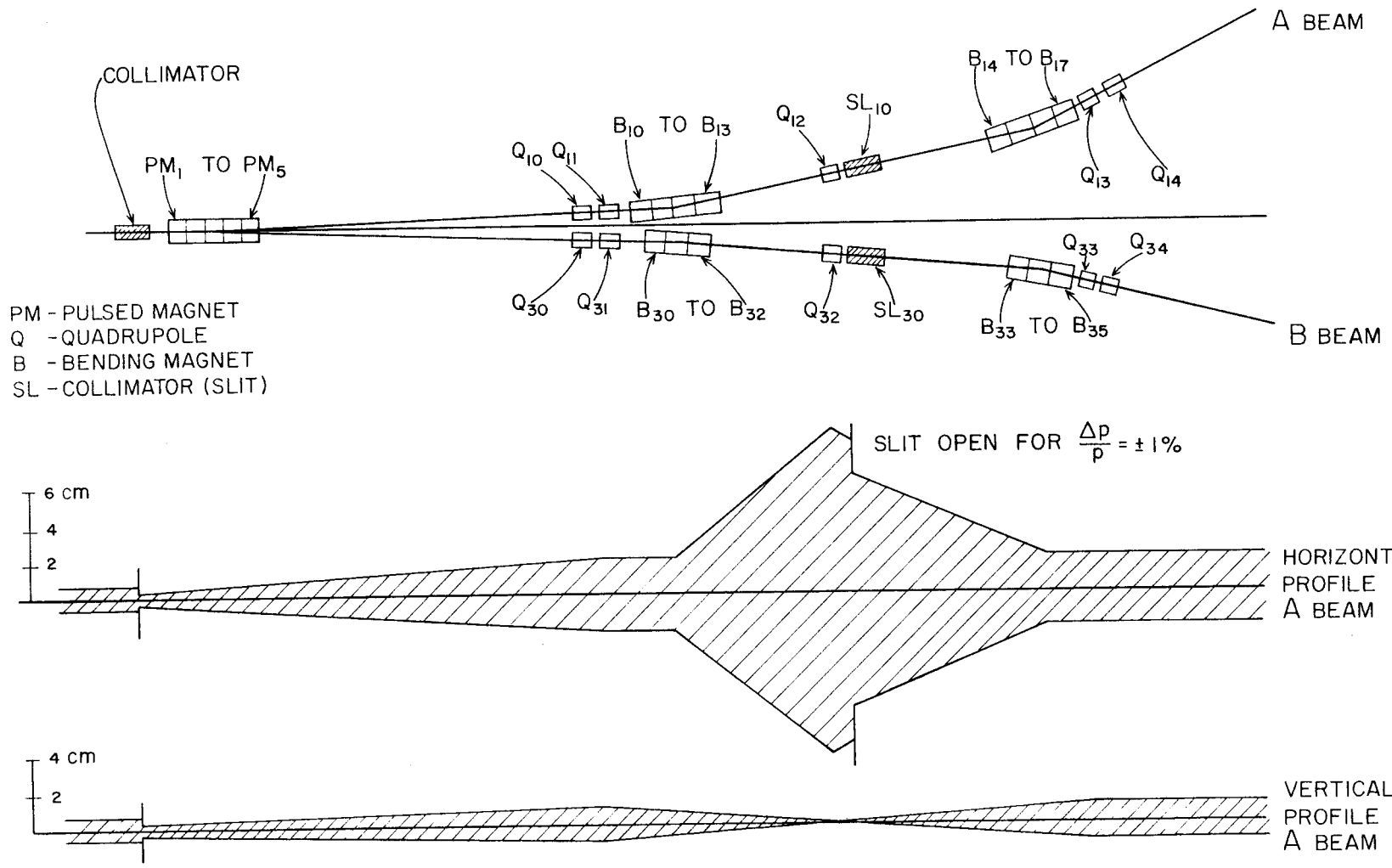

FIG. 1 SCHEMATIC LAYOUT OF THE BEAM SWITCHYARD AND PROFILES OF THE A BEAM

159-1-8

design and construction of the magnet are described by H. Brechna.[1]

The design of the vacuum chamber for the electron beam through the magnet requires special attention because the selection of the chamber material is critical for trouble-free operation. (See Appendix A.) If the vacuum chamber is made of a conductive material, the eddy currents induced in the vacuum pipe can cause excessive power loss and the generated heat in the pipe might result in outgassing in the chamber. If the beam pipe is built from insulating materials such as ceramic, epoxy, or glass, then radiation damage (see Appendix A) and the surface charge build-up which can result in breakage in the pipe would seriously limit the lifetime of the pipe. The most reasonable choice for the beam pipe in the pulsed magnet is metal-coated ceramic pipe; a ceramic pipe would eliminate excessive power loss, and the conductive surface would prevent surface charge build-up.

The third problem, that of designing a pulser to pulse the required energy into the magnet, will be discussed in the following sections.

The magnetic field required to switch an electron beam of $E = 25$ GeV through an angle $\alpha = \pm 0.5^{\circ}$ can be calculated from the equation (see Appendix B):

$$\int_{0}^{z_{o}} B(z)\, dz \approx n\, B_{o}\, (\ell + 2g) = \frac{\alpha(\text{radian})}{300} E\ (\text{MeV})$$

$$= 0.73 \left(\frac{\text{weber}}{\text{meter}} \right)$$

where n is the number of magnets in the deflection system, ℓ is the length of each magnet, and g is the half-gap length. For the required deflection, the stored energy in the field is

$$E_{m} = \frac{1}{2} \int HB\, dV = 530 \text{ joules}$$

or, by neglecting the effect of the fringing field, the stored energy in the gap can be expressed with the following approximate formula

$$E_{m} \approx \frac{1}{2} \mu_{o}\ H^{2} \ell g w$$

where ℓ is the length of the gap, g is the height of the gap, and w is the width of the gap.

In order to prevent the stored energy and thus the pulser size from being larger than necessary, the dimensions of the gap should be kept as small as possible. The minimum size of the gap height g is restricted by the size of the vacuum chamber necessary to transport the beam through the magnet. The minimum size of the width is restricted because a certain width-to-height ratio is necessary in order to obtain a homogeneous field inside the magnet gap.

The stored energy for a given deflection can be expressed as

$$E_m = \frac{B^2 \ell w h}{2\mu_o}$$

and with

$$\int_0^{z=\ell} B\, dz \approx B\ell = 0.73 \left(\frac{\text{weber}}{\text{meter}}\right),$$

E_m can be written in the following form

$$E_m = \left[\frac{wh(0.73)^2}{2\mu_o}\right] \frac{1}{\ell} = K \frac{1}{\ell} \qquad \text{where } K \text{ is a constant,}$$

which shows that if the deflection magnet is longer, less stored energy is required in the magnet gap for a given deflection.

In order that the stored energy in the magnetic field might be minimized while the deflection and the length of the path are kept constant, R. F. Mozley[2] calculated the length of the deflection magnet as a function of the stored energy in the magnetic field. The optimum length necessary was calculated to be 60 meters. Because of this long optimum length, which would make the system very costly, a practical choice for the magnet is appreciably smaller than that given by the requirement for optimum energy storage. The magnet actually designed uses five 1-meter sections and is powered by pulsed high voltage supplies (modulators); each magnet is excited by two modulators, one for each polarity. The magnet can

switch the beam into either of two target areas at any repetition rate up to 360 pps.

With $n = 5$, $\ell = 0.85$ meter, and $2g = 5$ cm, the peak magnetic field is

$$B_o = 0.17 \text{ (weber/meter}^2\text{)}$$

The modulators are required to supply 106 joules to each of the five magnets 360 times a second.

II. OPTICAL PROPERTIES OF THE PULSED MAGNET SYSTEM

The accuracy requirements of the magnetic field in the switching magnet can be estimated from the optical properties of the deflection system.

The optical transfer matrix for the deflection system from the exit of the pulsed magnet to the energy defining slit has the form

$$\underbrace{\begin{pmatrix} X \\ \theta \end{pmatrix}}_{\substack{\text{quad} \\ \text{input}}} = \begin{pmatrix} M_{11} & 0 \\ M_{21} & M_{22} \end{pmatrix} \underbrace{\begin{pmatrix} X_o \\ \theta_o \end{pmatrix}}_{\substack{\text{machine + pulsed} \\ \text{magnet output}}}$$

which shows that a change in the input divergence angle θ_o into the deflection system does not change the focusing condition or the energy resolution in first-order optics. This means that the deflection system is decoupled from the pulsed magnet and the accelerator, and a change in the divergence angle due to a small amplitude variation in the magnetic field of the pulsed magnet will not influence the focusing conditions. The limit for the maximum variation in θ_o is set by the aperture size of the input quadrupole of the deflection system. Because the half-aperture size is 4 cm and the half-beam width is 2 cm, the offset distance for the beam should be less than ±2 cm. However, the change in the offset distance b is proportional to the change in magnetic field. The maximum for this system can be calculated from the formula

$$\delta b(\text{cm}) = 8000 \times \frac{0.5}{57} \times \frac{\Delta B}{B}$$

If $\delta b = \pm 2$ cm, then $\Delta B/B = 2.65 \times 10^{-2}$; using for the peak field B = 1700 gauss, it can be seen that the field in the pulsed magnet can change ±45 gauss. This number, however, is an order of magnitude value only, because this calculation does not take into account the finite beam divergence from the accelerator,[3] the effect of possible asymmetries in the rf circuit for the acceleration guide,[4] the possible radial electrical fields in the waveguide,[4] and the misalignment of the whole accelerator. Because of the statistical nature of these effects, an accurate calculation of the beam divergence angle caused by the variation of the field in the pulsed magnet cannot be made.[5] In order to minimize the beam divergence and the phase space introduced by the pulsed magnet system, the pulsed magnet modulators will be regulated so that

$$\sigma\left(\frac{\Delta B}{B}\right) \approx 1 \times 10^{-3}$$

or 0.1%. A detailed argument supporting the 0.1% field variation requirement in the pulsed magnet is presented in Appendix C.

III. CIRCUIT REQUIREMENTS

The pulser circuit must be capable of pulsing the pulsed magnets with enough current to bring the field in the gap to approximately 2000 gauss and to hold the field constant during the 2 microseconds that the beam passes through the magnet.

In order to pulse a magnet current to a specific value and hold the current constant, it is necessary that a high voltage be applied during the rise time and that the voltage during the top of the pulse be reduced to a value that will supply the resistive losses. A negative pulse is then required to bring the current back to zero (see Fig. 2a). A vacuum tube circuit could be used to produce the waveforms as shown in Figs. 2a and 2b, but the losses in the tubes would be very high because of the high current that is necessary. The waveforms shown in Figs. 2c and 2d can be produced by connecting a charged capacitor across the magnet.

The magnet current in Fig. 2c, being a sine wave, is approximately flat during the time when the two-microsecond beam pulse passes throuth the

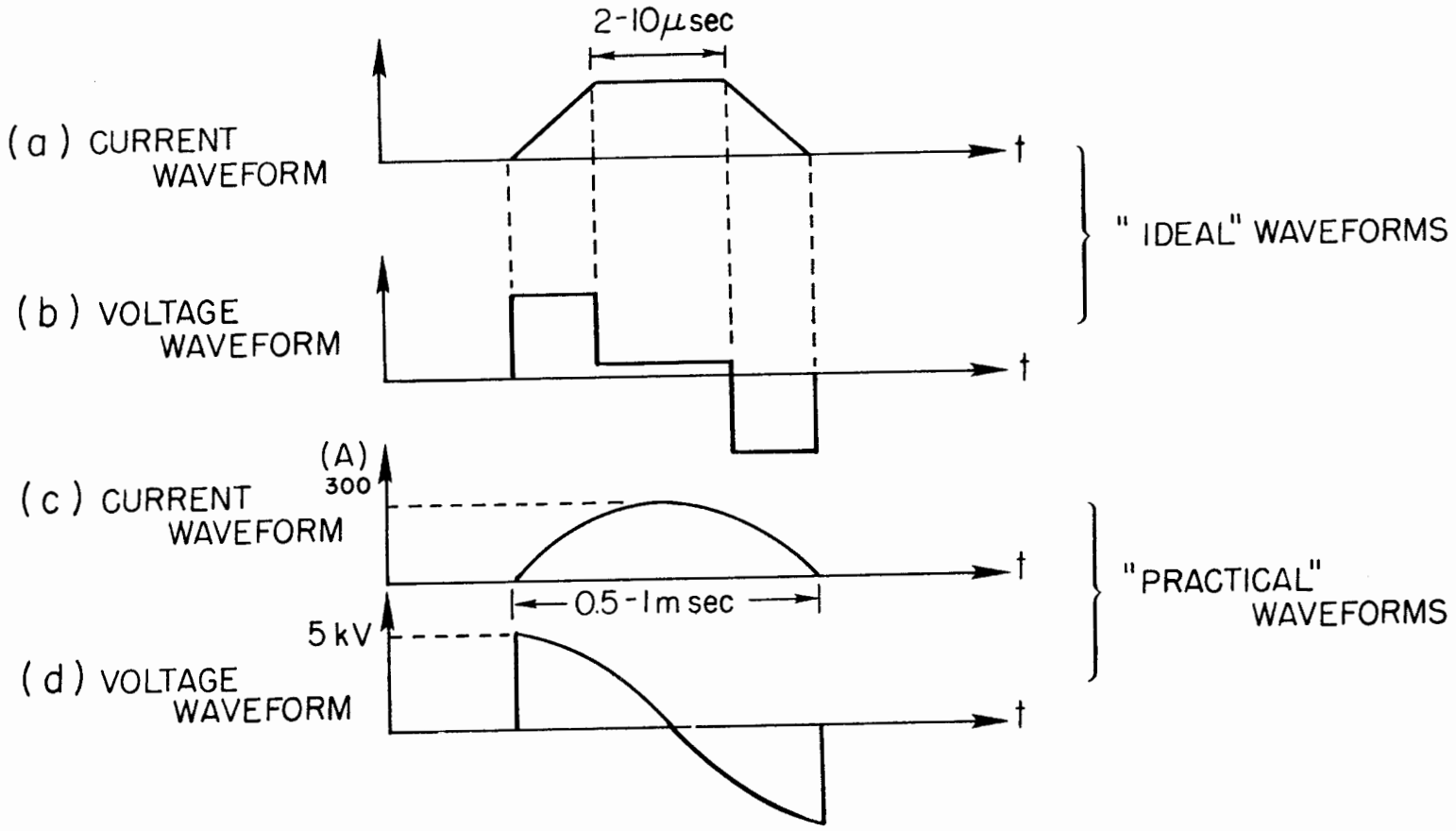

212-2-A

FIG. 2 IDEAL AND PRACTICAL WAVEFORMS FOR THE MAGNET PULSER.

magnet. An amplitude error of 0.1% occurs at 2.5° on either side of the peak of a sine wave. A natural frequency of 1 kc would therefore be flat to 0.1% for 14 microseconds.

Although a circuit that connects a charged capacitor across the magnet will produce the desired current waveform, it leaves the capacitor charged to the wrong polarity at the end of one-half cycle. Another switch is then necessary to place the capacitor across the magnet again in order to reverse the polarity of the capacitor. The polarity reversal can also be accomplished by connecting the capacitor across a dummy coil (Fig. 3). There are several advantages to using a dummy coil to reverse the capacitor voltage. The heat losses in the magnet are cut in half because current flows through the magnet only once per cycle. Because the magnet may be placed a long distance from the pulser and the dummy coil can be placed close to the pulser, losses in the cable can be reduced. The problem of eddy current losses in the vacuum chamber gap is reduced by using a dummy coil because the number of pulses of current flowing in the magnet is cut in half.

A. Energy Recovery

It is desirable in a magnet pulser to recover as much of the energy as possible. If 500 joules of energy were dissipated during each pulse, 360 pulses per second, the average power dissipated would be 180 kW. This amount of power is not only an expensive waste but would also require a large cooling system to remove the heat. It is desirable, therefore, to have a pulser circuit that can recover as much of the energy as possible from the magnet and store it to be used for the next pulse.

The circuit shown in Fig. 3 was chosen as the basic circuit to be used to build the prototype magnet pulser.

B. Choice of Switch Tubes

After selecting the basic circuit, there remains the problem of selecting the proper switching devices. The basic requirements of the switch are that it be capable of holding off 5 kV in both the forward and reverse directions and be able to switch approximately 300 amps when triggered on. Some possible choices that were considered were vacuum tubes, thyratrons, silicon-controlled rectifiers, and ignitrons.

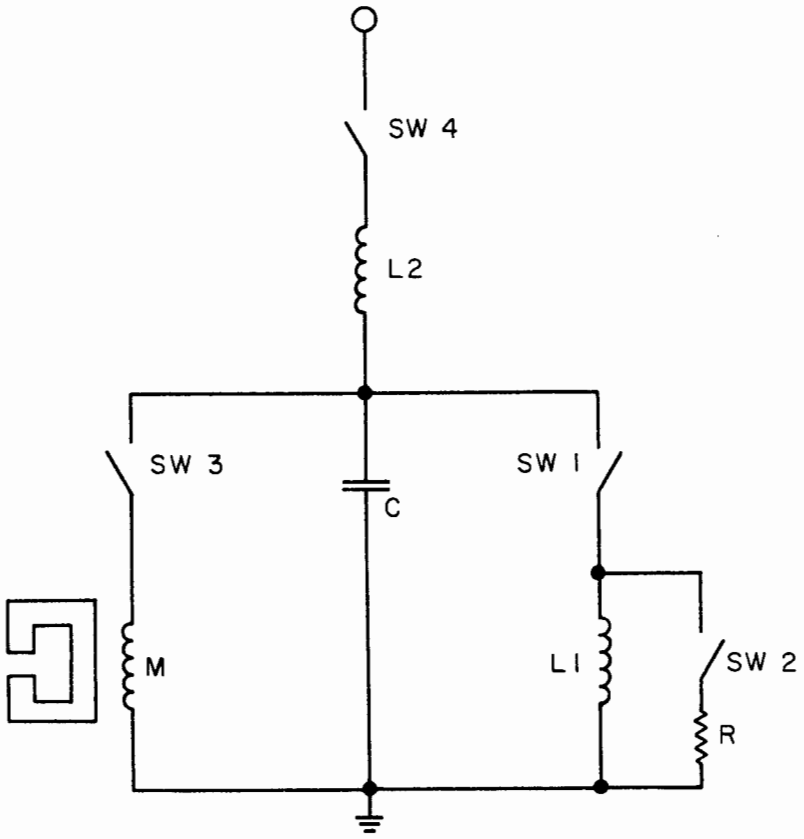

$C = 10\ \mu F$

$L_1 = 2.4\ mH$

$M = 2.4\ mH$

$L_2 \approx 1\ mH$

FIG. 3 MAGNET PULSER CIRCUIT DIAGRAM

159-2-A

Because of the high voltage drop, a vacuum tube switch would dissipate a large amount of power and was therefore not considered a good choice.

A thyratron is capable of switching large currents very efficiently if the pulse width is on the order of several microseconds or less, but the requirement that the switch carry a large current for one millisecond eliminated the possibility of using a thyratron. The lifetime of the thyratron cathode would be greatly decreased in the large duty cycle operation due to the positive ion bombardment of the cathode surface.

Silicon-controlled rectifiers can switch large currents and long pulses; however, at the time of writing, the maximum voltage rating on silicon-controlled rectifiers requires that several be stacked in series in order to hold off 5 kV. Silicon-controlled rectifiers could be used; however, ignitrons seemed to be a much better choice because there is a type of ignitron available which is capable of holding off voltages much higher than 5 kV and is able to switch the long pulse of high current required. In Appendix D the theoretical reasons are summarized for the selection of the gridded ignitrons as switch tubes.

IV. DESCRIPTION OF THE MAGNET PULSER CIRCUIT

A. General

The pulser can be described as an RLC circuit which is operated by closing a series of switches in the proper sequence (see Fig. 3). The switches are ignitrons that are turned on with trigger pulses and are turned off when the current tries to reverse direction through them.

The operation of the circuit is as follows: Capacitor C is charged to 5 kV (Figs. 3 and 4), and at time t_1, SW1 is closed; L1 and capacitor C begin to ring with a natural frequency of 1000 cps (see Fig. 5), and the polarity across capacitor C reverses. As the voltage across capacitor C approaches -5 kV, it is monitored by a comparator which produces a trigger pulse when the capacitor voltage reaches the desired level. The trigger pulse from the comparator closes SW2. Closing SW2 places a resistor across L1 and diverts the remaining current through this resistor, thereby preventing capacitor C from charging any further. SW1 becomes reversed-biased and opens.

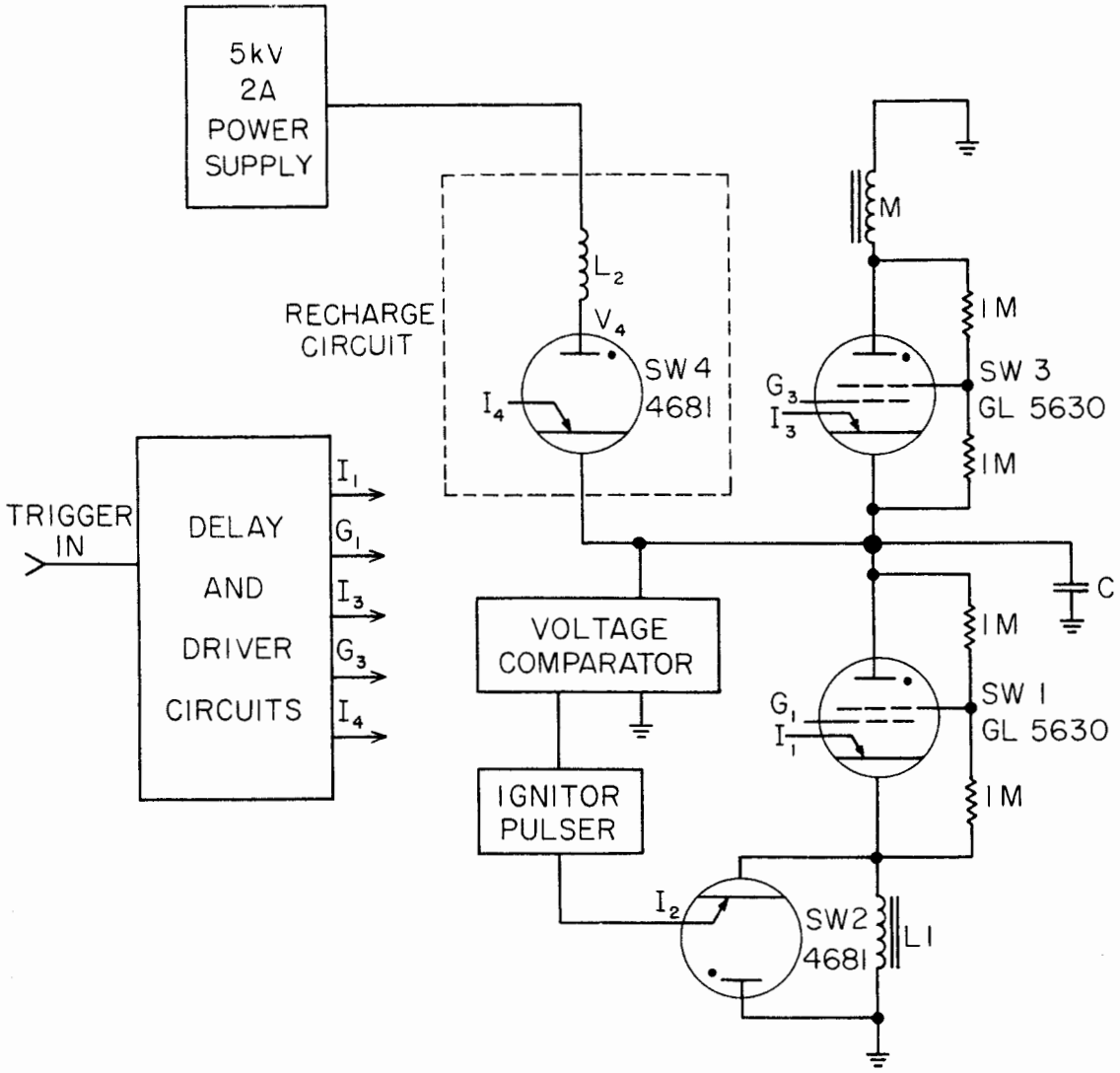

FIG. 4 MAGNET PULSER

159-3-A

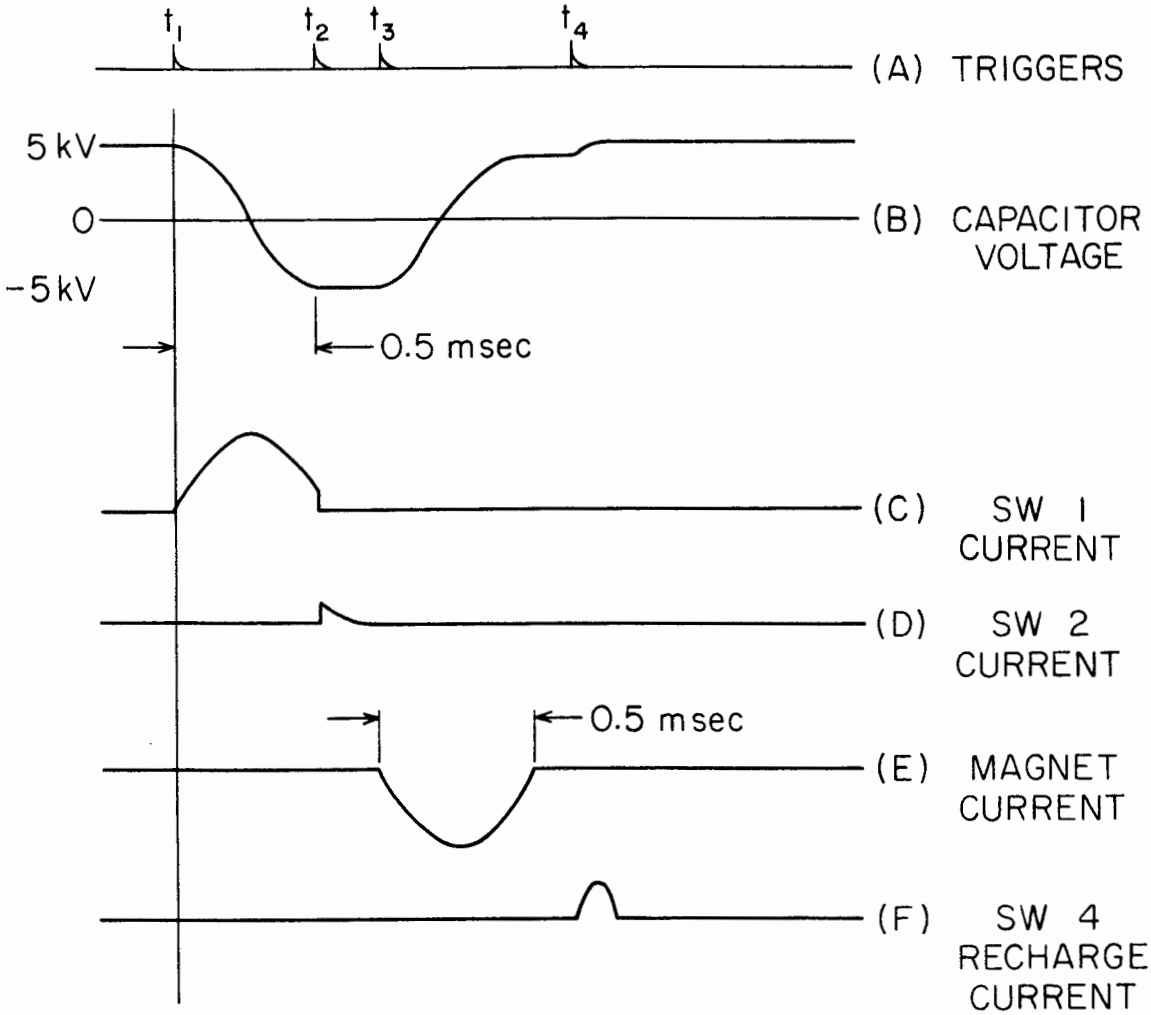

FIG. 5 WAVEFORMS

159-4-A

With the capacitor charged to an accurately known voltage, the pulser is now ready to pulse a precise amount of energy into the magnet **M** by closing SW3.

SW3 is closed at time t_3 (Fig. 5). The current through the magnet reaches its peak value at the time when the beam passes through the magnet. At the end of one-half cycle of magnet current the capacitor is recharged to a positive voltage and SW3 opens. SW4 is now closed and the capacitor recharges to its initial value, and the cycle is complete.

B. Major Components

The major components of the pulser (see Fig. 4) are the ignitron switch tubes, the storage capacitor C, and the recharge circuit with the power supply.

1. Switch Tubes

The switch tubes (SW1, SW3) must be able to hold off 5 kV when off and carry 300 amps when triggered on. As mentioned previously, ignitrons were chosen because they are capable of conducting long pulses of high current with low tube losses. Gridded ignitrons are required because it is necessary for the switch tube to hold off high voltage immediately after it has conducted a high current. Tests on tubes without grids showed that they did not recover their voltage hold-off capability for several milliseconds after conducting.[6] Because SW2 and SW4 (Fig. 4) do not carry high peak currents, it is not necessary that they be gridded tubes.

2. Storage Capacitor

The storage capacitor consists of a 10-μF capacitor bank that is charged to both plus and minus 5 kV 360 times per second. The capacitors therefore carry current 720 times per second. The rms current rating of the capacitor must be approximately 150 amps and the voltage rating plus and minus 5 kV. The waveforms of the capacitor voltage and current are shown in Fig. 5.

3. Recharge Circuit

The recharge circuit consists of a charging reactor in series with an ignitron. Because the pulser operates with a large duty cycle, the storage capacitor has to be recharged with a triggered charging tube during the interpulse period. The recharge tube conducts a small current

compared to the main switch tube; therefore, a gridded tube is not required to hold off the voltage.

The average current carried by the charging tube is approximately 2 amps when the pulser is run at full power. Two amps average is well below the current rating of many ignitrons that are commercially available; however, most of the ignitrons without grids are not rated for high voltage. The ignitron used for the recharge tube, a WL 4681, was designed for high voltage service as a capacitor discharge tube. The high voltage rating does not apply to a tube that has recently conducted a large current; therefore, the WL 4681 is not acceptable for use as the main switch tubes (SW1, SW3).

C. Timing and Trigger Circuits

The circuits used to provide the trigger pulses to the ignitrons are shown in Fig. 6. Each of these circuits consists of seven delay circuits, three triggered power supplies, four ignitor firing circuits, and two ignitron grid pulsers.

1. Delay Circuit

A typical delay circuit is shown in Fig. 7. The delay circuit is a standard monostable multivibrator circuit; however, care was taken to use a circuit that would recover quickly because some of the delays must operate with a large duty cycle.

2. Ignitor Firing Circuit

The ignitor firing circuit (Fig. 8) is used to pulse the ignitors of the ignitrons. Ignitors require approximately 1/2 to 1 joule of energy per pulse to fire reliably. This energy is stored in the 8-μF capacitor (Fig. 8) by resonant charging the capacitor through L1 from the 200-volt triggered power supply. When the silicon-controlled rectifier (SCR) is triggered by the delay circuit, a negative pulse is developed at the output of this circuit. The transformer serves to invert the negative pulse as well as to isolate the SCR circuit from the floating cathode potential of the ignitron (5 kV).

The ignitor-to-cathode resistance is only a few ohms before the ignitor fires and drops to a much lower value (a few milliohms) when the ignitor fires. Because the process known as firing is a breakdown process, a high voltage (300 volts - 1 kilovolt) is required to fire the ignitor.

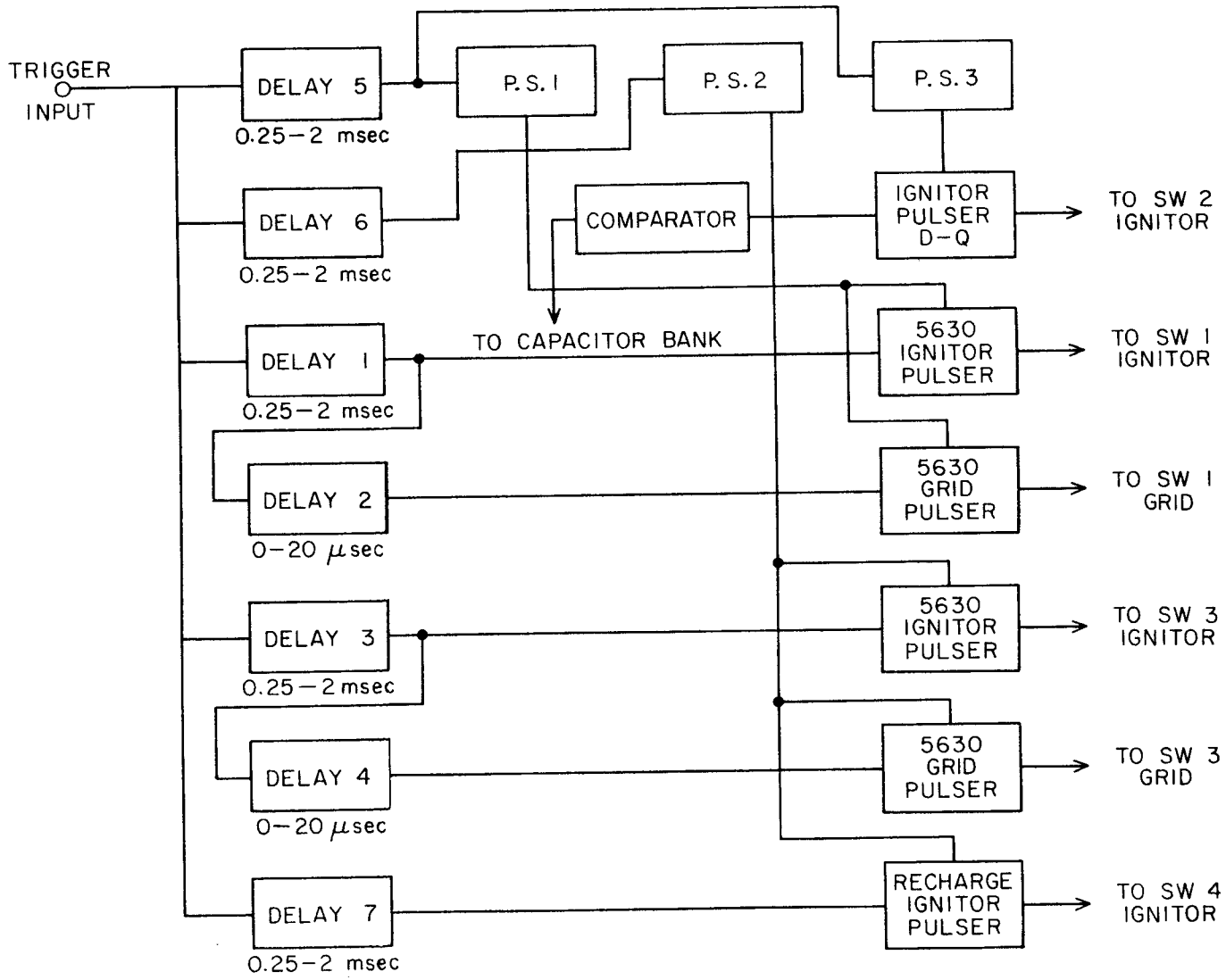

FIG. 6 TRIGGER CIRCUIT

159-5-A

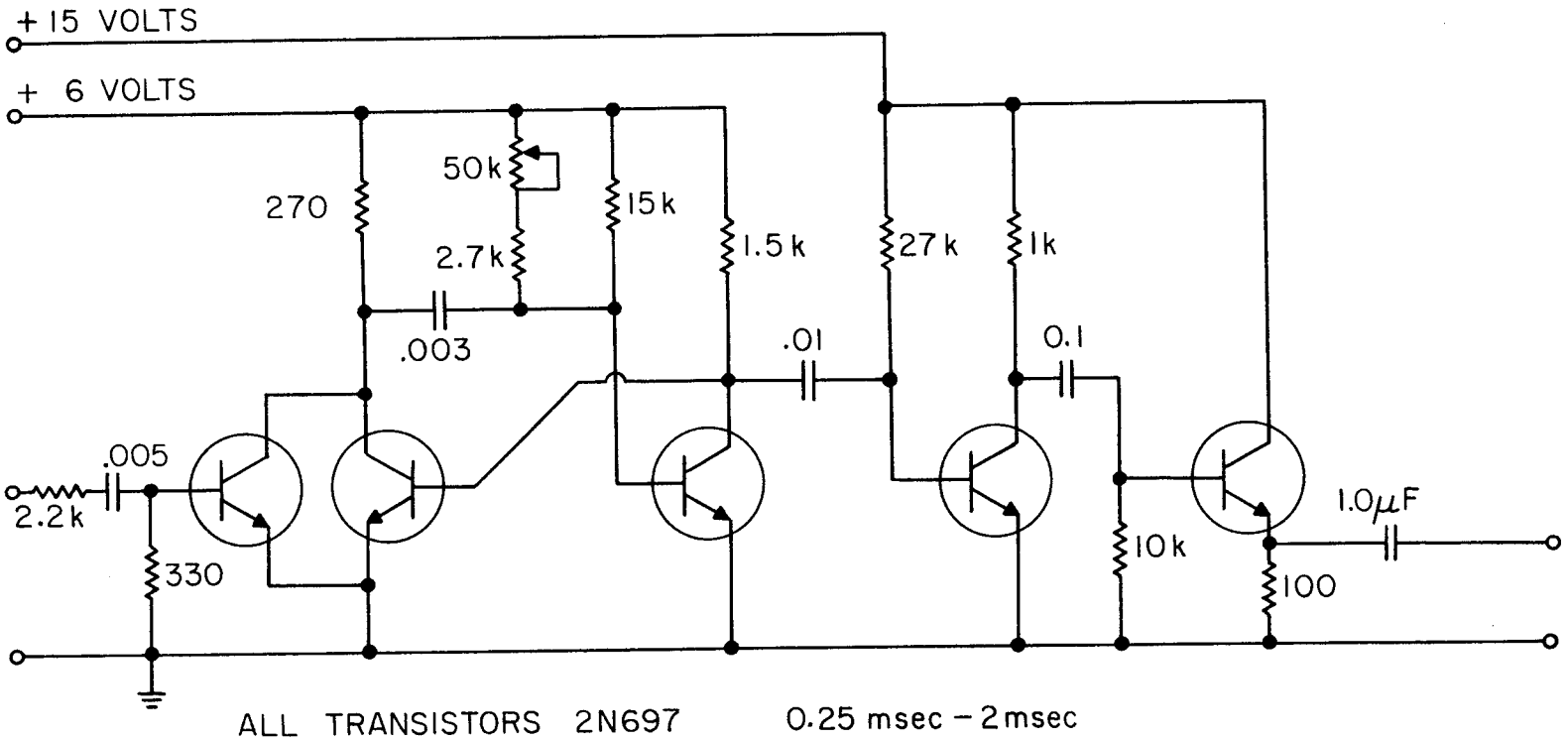

FIG. 7 DELAY CIRCUIT

159-6-A

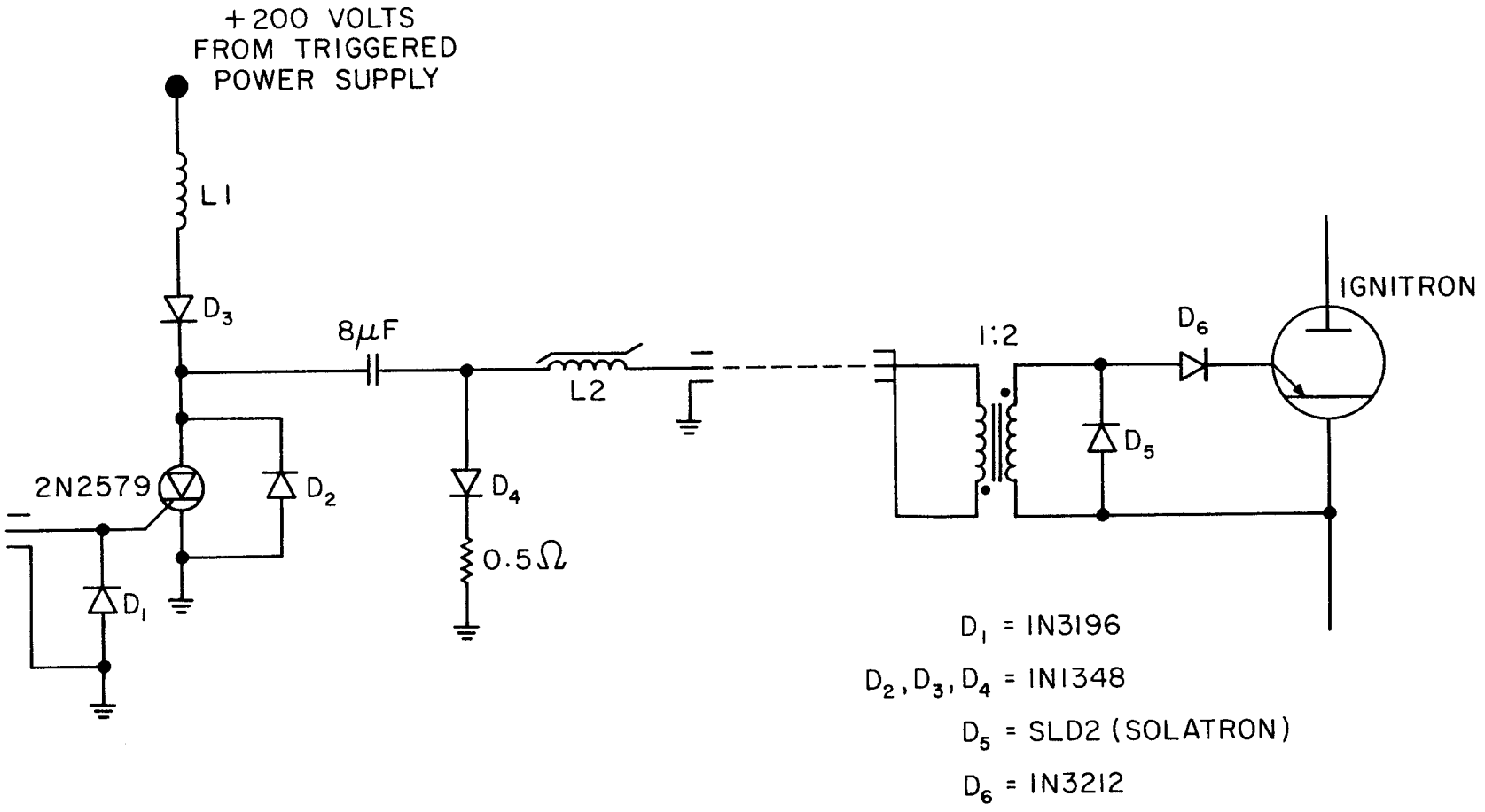

FIG. 8 IGNITOR PULSER CIRCUIT

159-7-A

The ignitor as a load for the firing circuit thus looks very much like a spark gap which is shunted by a few ohms. Therefore, the firing circuit must be a low impedance, high voltage source.

A charged capacitor which is connected by a switch (SCR) across the ignitor-to-cathode terminals is a high voltage, low impedance source for a few microseconds and will fire an ignitor if the capacitor contains enough energy (approximately 1/2 to 1 joule).

Because the cathodes of the main switch tubes (Fig. 4) are floating at a high voltage above ground (±5 kV) it is necessary to isolate the ignitor firing circuit from the cathode potential with a pulse transformer. It is necessary that the pulse transformer have a very low value of leakage inductance. If too much inductance is inserted between the firing circuit and the ignitor, it is difficult to get the voltage across the ignitor to rise fast enough to fire the ignitor.

One type of pulse transformer that has a good coupling coefficient and will pass relatively long pulses with fast rise times is a coaxial transformer. The coaxial transformer that was designed for the ignitor firing circuits consists of ten turns of (RG8U) cable wound on an Arnold AL 118 core. The center conductor was used as the secondary and the shield was used as the primary.

Although it is desirable to keep the inductance between the ignitor and its firing circuit low, a small, saturable reactor (L2 - Fig. 8) was placed in series to reduce the dissipation of power in the SCR during its turn-on time. An SCR is a very efficient switch because of the low voltage drop across it when it is conducting. However, if it must conduct a large current during its turn-on time while there is a voltage drop across the SCR, it will dissipate a large amount of peak power. By placing a small saturable reactor in series with the SCR, the current is limited to a low value during the turn-on time and is allowed to rise to the full value when the core saturates. The turn-on time for the SCR used is less than 1/2 microsecond and the time required to saturate the core is approximately 2 microseconds. The saturable reactor consists of ten turns of #16 wire wound on a Ferroxcube No. K3.005.01 core.

The 8-μF capacitor used in the ignitor firing circuit must be capable of passing a large rms current because it is charged to 400 volts and then

discharged 360 times per second. The capacitor used in the prototype was a G. E. type 28F984 which was designed for use as a commutating capacitor in SCR inverter circuits.

The SCR is a 2N2579 and was chosen because it has a fusing factor I^2t of 285 amp^2-sec which allows it to be used in circuits requiring high peak currents.

The diodes D5 and D6 (Fig. 8) are to prevent the backswing voltage from the pulse transformer from appearing across the ignitor-cathode terminals. Inverse voltage greater than -5 volts on the ignitor causes the ignitor rod to wet with mercury and thereby shortens its life considerably.

3. The Grid Pulser

The grid pulser (Fig. 9) is very similar to the ignitor pulser described above, but the grid pulser is not required to deliver much energy to the grid circuit; all that is required is a fast rising pulse of approximately 350 volts to overcome the grid bias. This pulse is usually applied 5 to 20 μsec after the ignitor pulse.

4. Triggered Power Supply

The power supply for the grid pulser and ignitor pulser (Fig.10) is included in the timing circuits because it contains an SCR in its output which isolates the power supply from the pulser circuit until a trigger pulse is applied. By not applying a trigger to the power supply until approximately 200 microseconds before the trigger is applied to the ignitor pulser, the anode of the SCR in the ignitor pulser is at ground potential during most of the cycle, and is therefore not susceptible to noise pulses which could trigger the pulser at the wrong time.

Figures 11 and 12 show front and back views of the prototype magnet pulser.

V. TEST RESULTS

The power requirements of the pulser were tested by operating the pulser for eight hours using the prototype pulsed magnet for a load. During the test the voltage across the capacitor bank (10 μF) was adjusted to approximately 5.1 kV. The energy delivered to the magnet was therefore

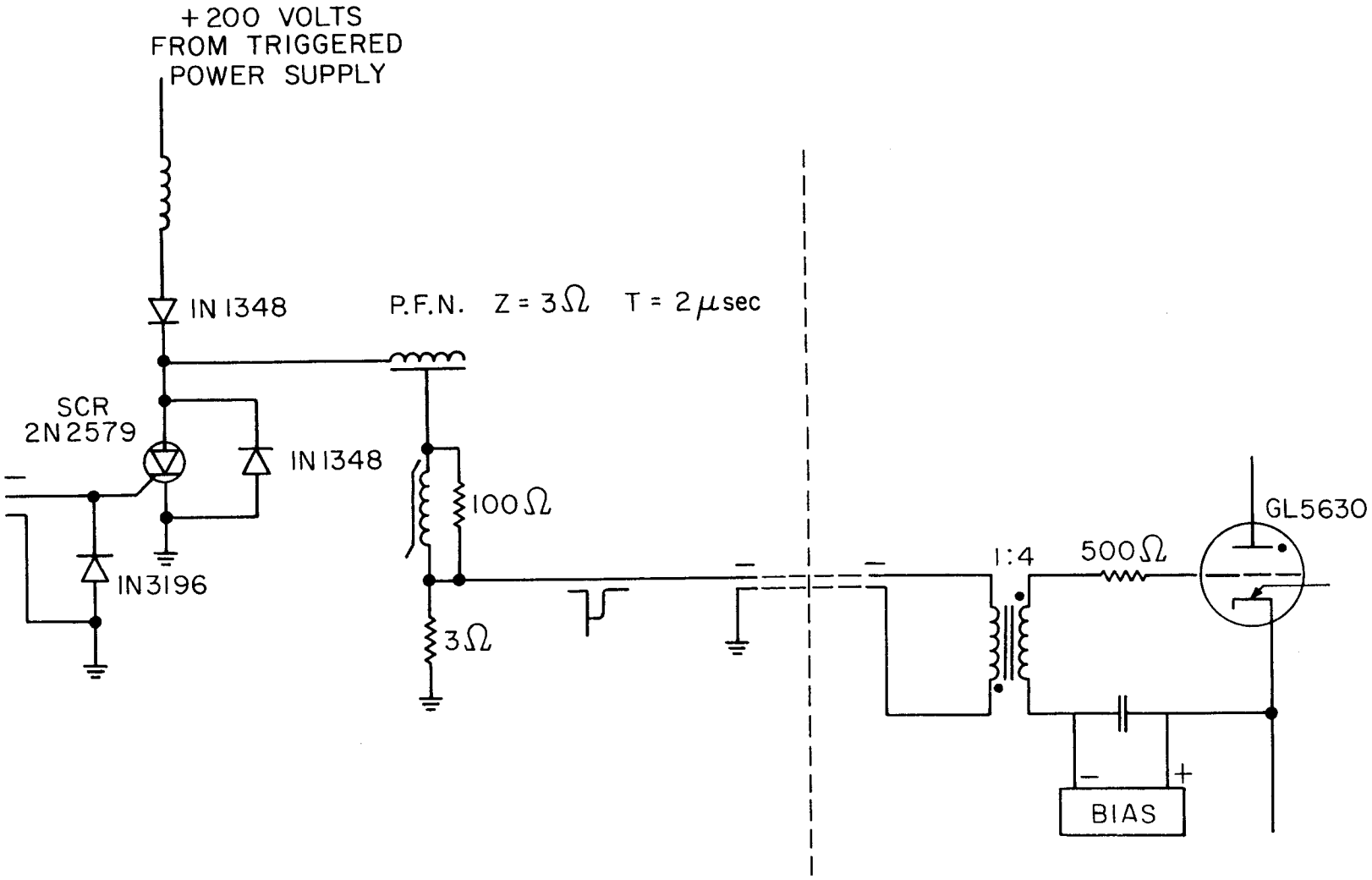

FIG. 9 IGNITRON GRID PULSER

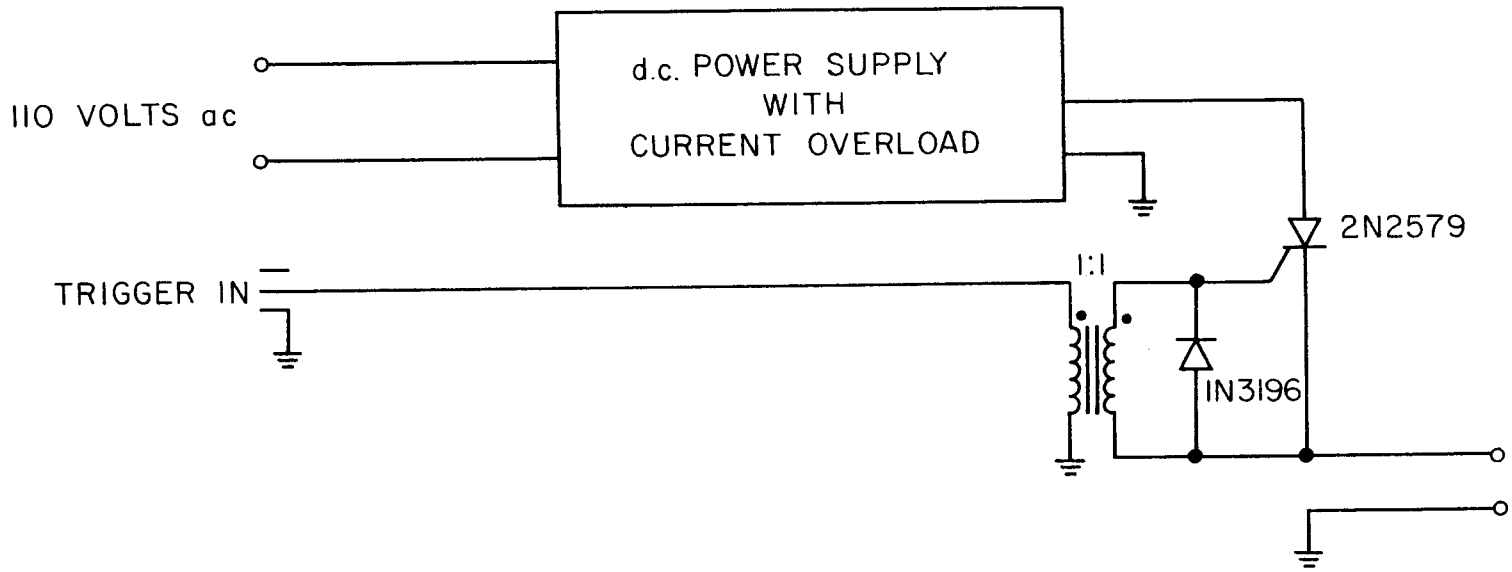

FIG. 10 POWER SUPPLY

159-9-A

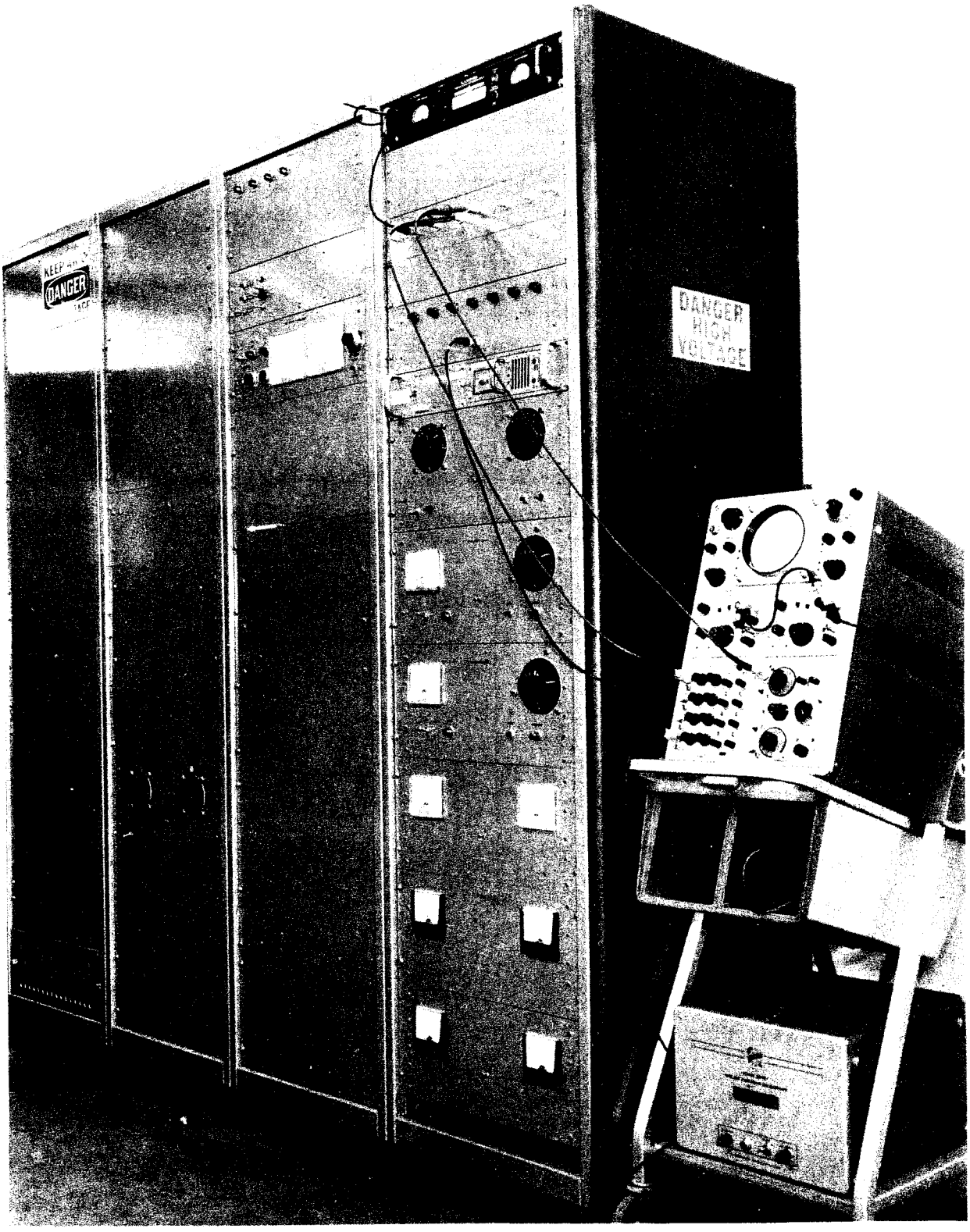
KEEP
DANGER
DANGER
HIGH
VOLTAGE

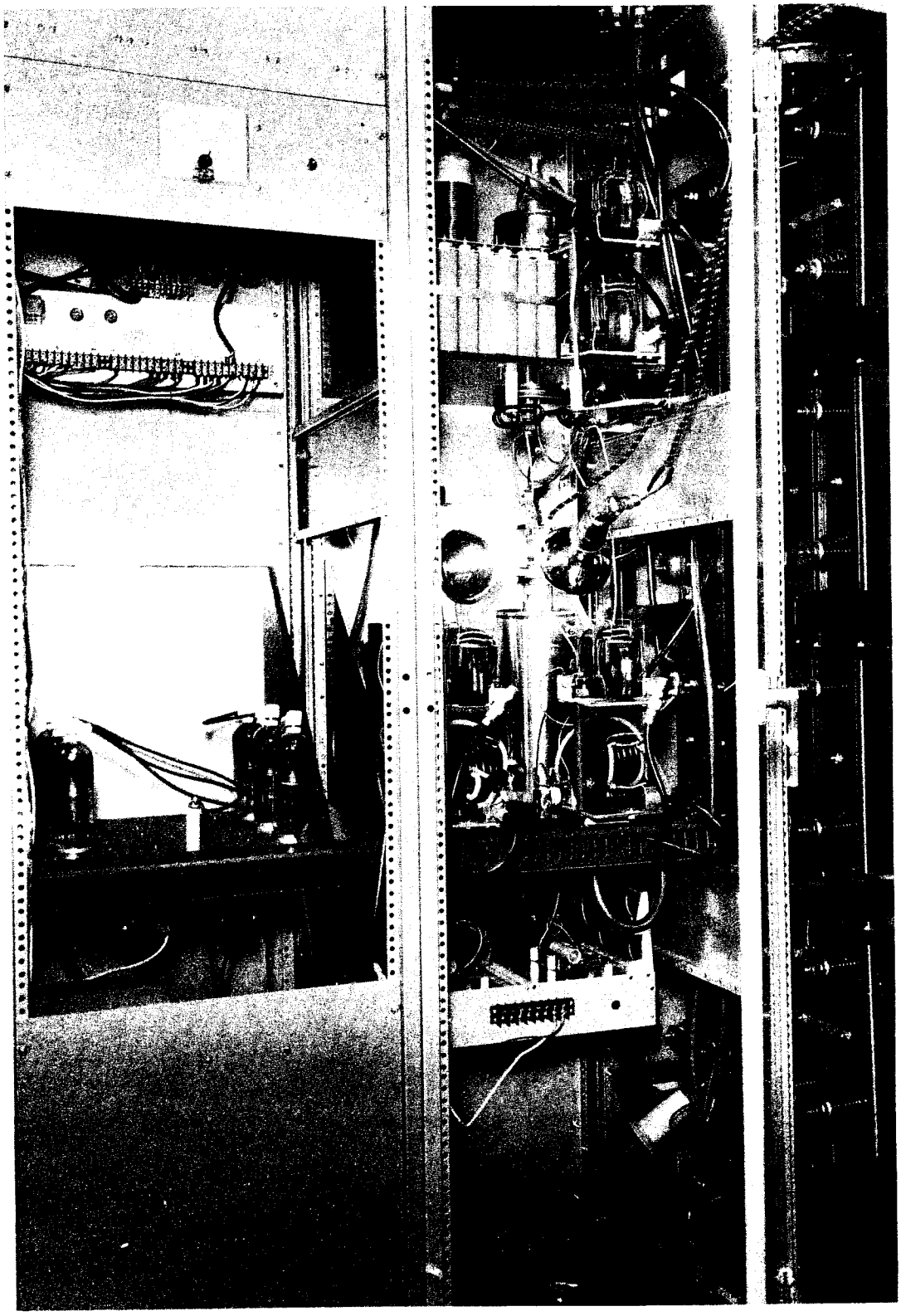

130 joules per pulse. The pulser was run for eight hours at 360 pulses per second without any failures.

The efficiency of the pulser was measured by observing the voltage across the capacitor bank before and after a complete cycle of operation. Eighty-five percent of the energy was recovered after each cycle while the pulser was running at full power and full repetition rate.

The accuracy of the Q-spoiling regulator circuit was tested by using a current monitor and a Tektronix Type Z preamplifier to measure the peak current in the magnet. The peak field was also measured with an EMR magnetometer.[7]

Using the above testing methods, an accuracy of ±0.1% was obtained; however, the results were difficult to repeat, and further tests indicated that the Q-spoiling regulator system could not be relied upon for an accuracy greater than ±0.25% with a line voltage change of ±2%.

Another method of regulation has been tested and was found to regulate to ±0.1% with a line voltage swing of ±3%. The regulator circuit is shown in Fig. 13. The circuit works as follows: SW5 is fired when the capacitor voltage is positive, causing the capacitor bank to discharge with a time constant of approximately 1 msec. When the voltage reaches a predetermined level, the comparator circuit produces a trigger which fires SW1, and the voltage across the capacitor bank reverses. Therefore, the voltage at which SW1 fires does not depend on the power supply voltage as long as the power supply voltage is greater than the voltage to which the comparator is set. The second stage of the regulator consists of a hard tube which conducts when the capacitor voltage is negative and is turned off by a comparator when the desired voltage is reached.

The first stage takes a line voltage change of ±5% and regulates to about ±½%. The second stage regulates the capacitor voltage to ±0.1%.

VI. FIELD MEASURING AND INTERLOCKING SYSTEM

To measure the magnetic field in the pulsed magnets, the field measuring and interlocking system shown in Fig. 14 was designed.[8,9,10] An interlock gate must enable the accelerator injector, if the peak field does not vary by more than ±1%. The system must send a 50-volt pulse

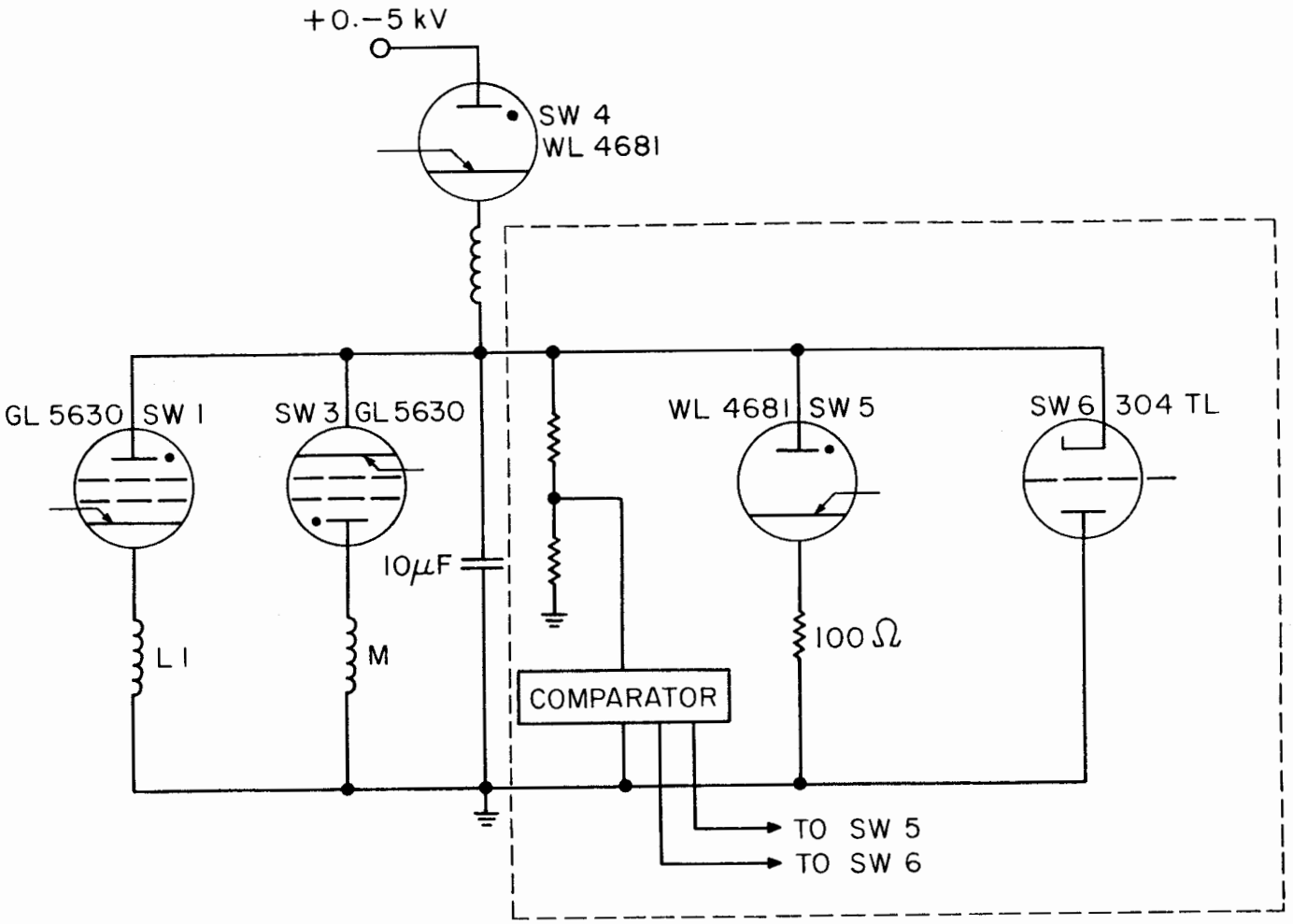

FIG. 13 TWO-STAGE REGULATOR

159-10-A

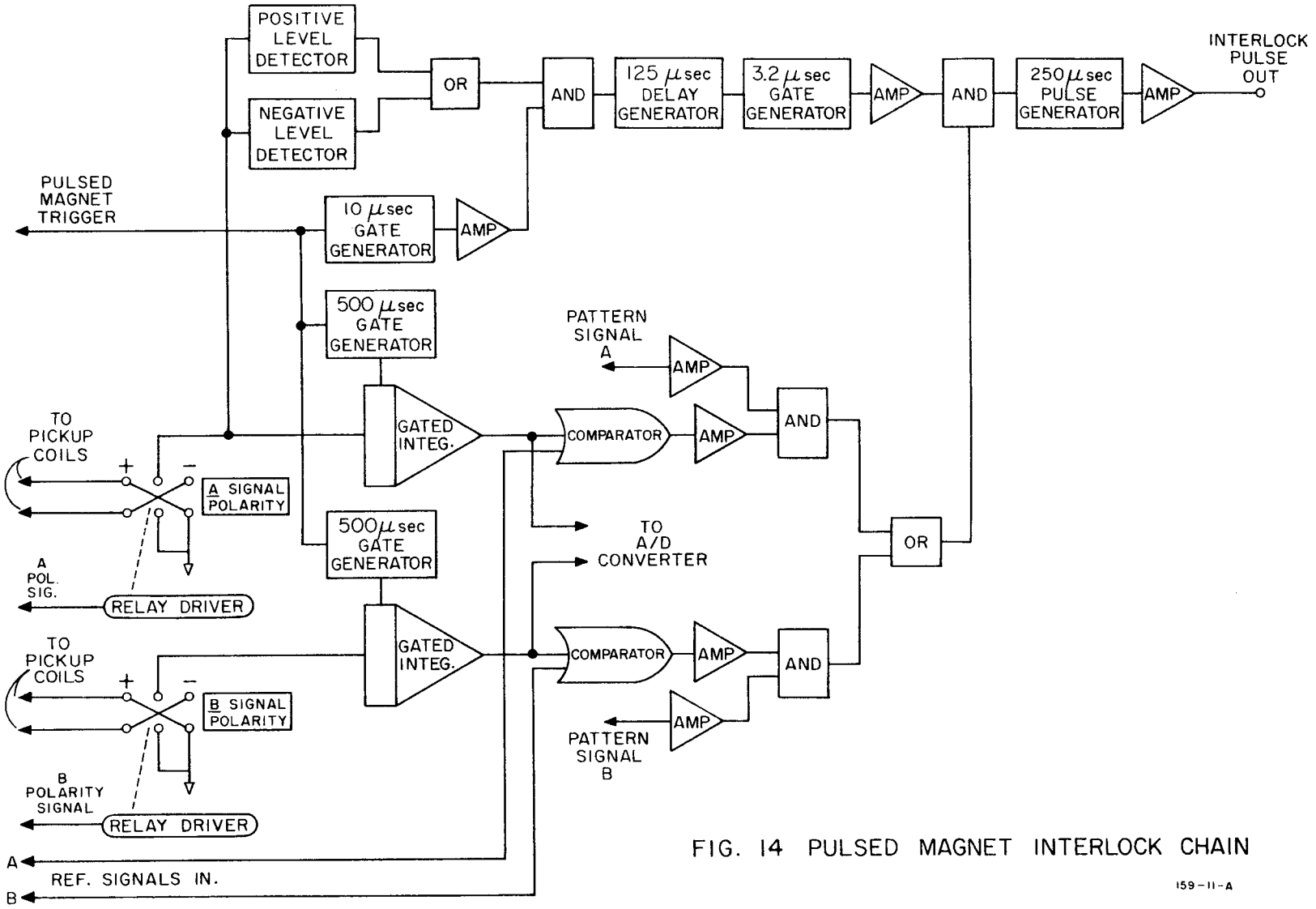

FIG. 14 PULSED MAGNET INTERLOCK CHAIN

159-11-A

(from 100 ohms) to the injector, rising no later than 150 μsec before the time of the next beam pulse; the pulse width must be at least 200 μsec, with rise and fall times less than 10 μsec. The interlock setting must track the bending magnet current.

The peak value of the field must be displayed to the operator on a four-digit illuminated display with an accuracy of 0.1% of reading or ±1 digit, whichever is greater.

The system in Fig. 14 operates as follows: The trigger to the pulsed magnet that initiates the magnet current pulse triggers a 10-μsec gate generator. When the pickup coils receive a signal, the positive (or negative) level detectors put out a pulse at the time the current pulse begins. If this pulse occurs within the 10-μsec gate interval, the pulse is gated through to the 125-μsec delay generator. This generator triggers a 3.2-μsec gate generator, forming at this point a 3.2-μsec gate which is delayed 125-μsec from the beginning of the current pulse.

In the meantime, the pulsed magnet trigger has also enabled a 500-μsec gate, which gates on the integrator. The integrator output is an accurate (0.1%) replica of the magnetic field waveform. A dc reference signal (derived from the bending magnet shunts) is set to be 70.7% of the desired peak value of the field pulse, and this reference voltage, along with the integrator output, is fed into an accurate comparator whose output is a pulse when the inputs compare within 1 millivolt. The comparator pulse is ANDED with the appropriate pattern signal and presented with the 3.2-μsec gate to an AND circuit.

The AND circuit, therefore, will produce an output signal when the field reaches 70.7% of the desired value 125 ± 1.6 μsec from the beginning of the field waveform. Because the field waveform is a sine wave, it is assured that the actual peak field is equal to the desired peak field within ±1%. The output signal from the AND circuit triggers a 250-μsec pulse generator which is amplified to 50 volts and presented to the 100-ohm line through a matching transformer. Fig. 15 shows the timing involved.

Two integrators with polarity switches are used because the comparators will operate on negative levels only. Thus the polarity switches are set so that the integrator outputs are always negative.

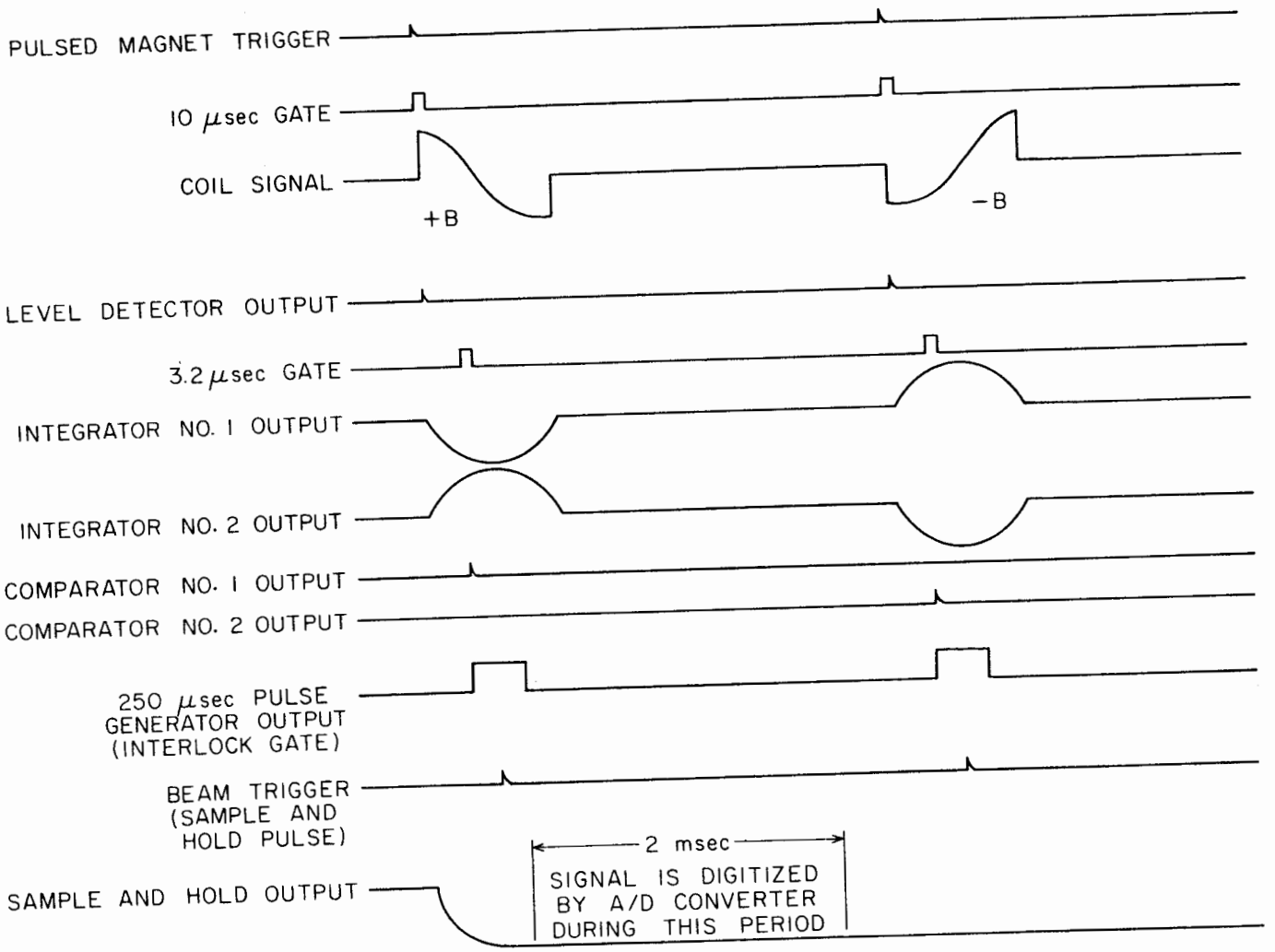

FIG. 15 INTERLOCK CIRCUIT TIMING DIAGRAM

159-12-A

Measurement of the magnetic field is accomplished by a sample-and-hold circuit and an A-D converter, corrected to the outputs of the integrators. A selector switch determines which of the two beams was measured; see Fig. 16 for circuit details.

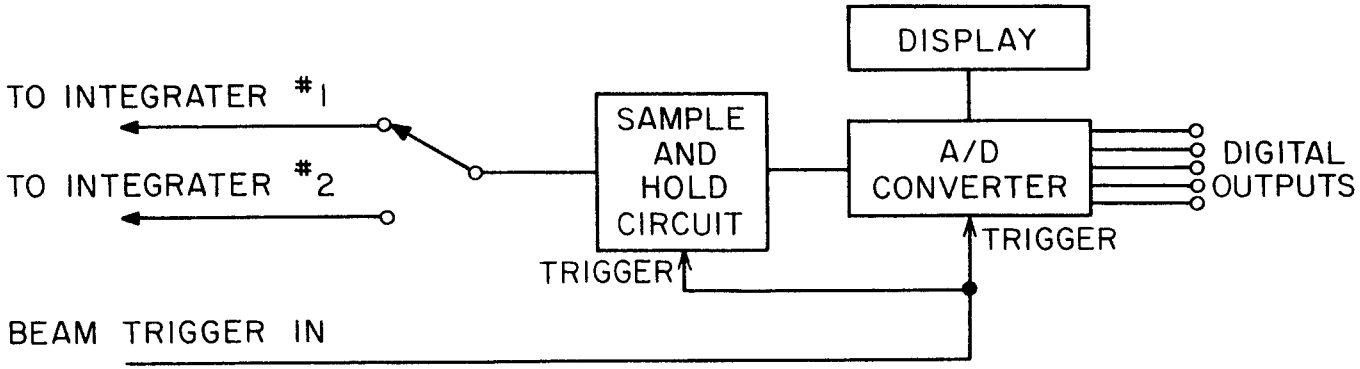

159-13-A

FIG. 16 MEASUREMENT SYSTEM

LIST OF REFERENCES

1. H. Brechna, SLAC Report No. 28, Stanford Linear Accelerator Center, Stanford University, Stanford, California (May 1964).
2. R. F. Mozley, Internal Report, Stanford Linear Accelerator Center, Stanford University, Stanford, California (March 1962).
3. C. H. Moore, S. K. Howry, and H. S. Butler, Internal Report, Stanford Linear Accelerator Center, Stanford University, Stanford, California (May 1963).
4. R. H. Helm and W.K.H. Panofsky, M-Report No. 201, Stanford Linear Accelerator Center, Stanford University, Stanford, California (November 1960).
5. H. DeStaebler, Jr., SLAC Report No. 9, Stanford Linear Accelerator Center, Stanford University, Stanford, California (November 1962).
6. J. L. Cole and J. J. Muray, SLAC Report No. 31, Stanford Linear Accelerator Center, Stanford University, Stanford, California (July 1964).
7. J. J. Muray and R. A. Scholl, SLAC Report No. 26, Stanford Linear Accelerator Center, Stanford University, Stanford, California (February 1964).
8. J. J. Muray, Internal Report, Stanford Linear Accelerator Center, Stanford University, Stanford, California (March 1963).
9. J. J. Muray and R. A. Scholl, Internal Report, Stanford Linear Accelerator Center, Stanford University, Stanford, California (August 1963).
10. R. A. Scholl, private communication.

APPENDIX A

RADIATION FIELD IN THE BEAM PIPE OF THE PULSES DEFLECTION MAGNET

The radiation in the beam pipe of the pulsed magnet comes in part from the beam collimator which is located at the exit end of the accelerator, and partly from synchrotron radiation of the deflected electron beam.

The beam current loss at the collimator is expected to be over 10% of the total current (40μA of average total current at 25 GeV). These scattered electrons will leave the collimator with energies ranging from zero to almost full energy, and with a divergence up to 10^{-3} radian. The expected beam radius in the pulsed magnet's vacuum chamber is

$$r_p \approx r_o + \ell\theta = 0.4 + 10^3 \times 10^{-3} = 1.4 \text{ cm}$$

where r_o is the beam radius before collimation and ℓ is the distance between the collimator and the pulsed magnet. It is evident from this that under normal circumstances the scattered beam from the collimator can pass through the vacuum chamber without hitting the walls. However, in a serious mis-steering of the beam, the scattered beam might hit the chamber wall and cause excessive damage.

The synchrotron radiation, which is tangential to the electron beam, normally will not hit the wall of the vacuum chamber; however, in the case of beam misalignment, the damage caused by this radiation could be very serious. To estimate the photon flux and a possible mechanism for radiation damage caused by synchrotron radiation, consider the energy loss for an electron moving in circle of radius R under the influence of a magnetic field B as*

$$\delta E = \left(\frac{4\pi}{3}\right)\left(\frac{e^2}{R}\right)\left(\frac{E}{mc^2}\right)^4$$

*J. Schwinger, Phys. Rev. 75, 1912 (1949).

or

$$\delta E_{keV} = \frac{88.5(E_{GeV})^4}{R(meter)}$$

where E_{GeV} is the electron energy in units of 1 GeV, R is the radius of the electron orbit in meters, and δE_{keV} is the energy radiated per revolution in units of 1 keV. For 0.5° deflection in the pulsed magnet, ℓ is 590 meters. For 25-GeV electrons the radiation loss would be

$$\delta E_{keV} = \frac{88.5(25)}{590} \approx 6 \times 10^4 \ \frac{(keV)}{turn}$$

However, the actual length of the electron trajectory in the pulsed magnet's vacuum pipe is only 1.35×10^{-3} times $2\pi R$. Therefore, the radiation loss per deflected electron in the magnet is

$$\delta E_{keV} \times 1.35 \times 10^{-3} = 81 \ \frac{keV}{deflection}$$

To estimate the average number of radiated photons, one has to calculate the average quantum energy, which is given by

$$\bar{\epsilon} = \frac{3}{2} \frac{\hbar c}{R} \left(\frac{E}{mc^2} \right)^3 = 6.3 \times 10^4 \ eV$$

Then the number of equivalent photons radiated by each deflected electron in the pulsed magnet is

$$N_{\bar{\epsilon}} = \frac{8.1 \times 10^4}{6.3 \times 10^4} = 1.28 \ \frac{photon}{deflected\ electron}$$

and the total number of photons radiated per second is the order of magnitude of 1.28×10^{14}, because the number of deflected electrons is 10^{14} per second. This relatively low energy photon flux might liberate electrons from the chamber wall with a quantum efficiency of 10^{-5} to 10^{-6}.

These electrons can form a surface charge on a non-conductive chamber wall and the high field strength (a few hundred volts/meter after a second of radiation) might cause electrical breakdown or cracking in the chamber wall when the lifetime of the surface charge is long enough and high surface density can build up. Therefore the non-conductive (ceramic) wall of the chamber should be coated with a thin metal film to prevent charge build-up without introducing excessive eddy-current losses.

APPENDIX B

CALCULATION OF THE MAGNETIC FIELD REQUIRED FOR A GIVEN DEFLECTION

The curvature of a charged particle moving in a magnetic field is given by

$$K = \frac{1}{r} = \frac{eB}{pc}$$

where e is the charge in electrostatic units, B is the magnetic induction in gauss, p is the momentum in cgs units, and c is the velocity of light in cm/sec. The curvature K is given in cm^{-1}, and it is the reciprocal of the radius of curvature.

Now one can relate the magnetic rigidity Br to the particle's energy by writing that

$$Br = \frac{Mvc}{e} = \frac{Mc^2\beta}{e}$$

where

$$\beta = \frac{v}{c}$$

Using the results of the relativity, namely that

$$E = Mc^2 = \frac{E_o}{\sqrt{1 - \beta^2}}$$

where

$$M = \frac{M_o}{\sqrt{1 - \beta^2}}$$

or

$$E = M_o c^2 + T$$

$$= E_o + T$$

where T is the kinetic energy, one can write that

$$\beta^2 = E^2 - E_o^2 = (E_o + T)^2 - E_o^2$$
$$= T^2 + 2E_oT$$

and with this

$$Br = \frac{E}{e}(T^2 + 2E_oT)^{\frac{1}{2}} \approx \frac{T}{e}\left(1 + \frac{1}{2}\frac{E_o}{T} + \ldots\right)$$

In practical units

$$Br = \frac{1}{300}(T^2 + 2T\,E_o)^{\frac{1}{2}} \left(\frac{\text{webers}}{\text{meter}^2}, \text{meter, MeV}\right)$$

or when $E_o/T \ll 1$, in the case of high energy particles, the rigidity can be expressed as

$$Br \approx \frac{T}{300} \left(\frac{\text{webers}}{\text{meter}^2}, \text{meter, MeV}\right)$$

When the particle moves in a magnet, then $\ell = \alpha r$ where α is the deflection angle and ℓ is the length of trajectory in the magnet. If α is small, the length of the trajectory is approximately equal to the length of the magnet, and one can write that

$$\int_o^\ell B(z)\,dz \approx \frac{\alpha}{300}T$$
$$\approx \frac{\alpha(\text{radian})}{300}E\ (\text{MeV})$$

which is the formula used to calculate the line integral of the field strength for a given deflection.

APPENDIX C

ESTIMATION OF THE MAGNETIC FIELD REGULATION REQUIRED IN THE PULSE DEFLECTION MAGNET

One way to estimate the field stability in the pulsed magnet is to try to separate from the total beam divergence θ_o, the divergence due to the accelerator itself (θ_1) and the part which is due to the pulsed magnet (θ_M). Computer calculations have verified that to achieve a 0.3-cm image spot at the collimator, the total divergence of the beam should be less than 3×10^{-4} radian. For a point spot the maximum possible divergence is 4.2×10^{-4} radian. In order to estimate θ_M, let us suppose that the beam has a gaussian intensity distribution at the end of the accelerator. Let $\sigma\theta_1$ be the standard deviation of the beam divergence before the pulsed magnet, $\sigma\theta_o$ be the standard deviation of the total beam divergence after the pulsed magnet, and $\sigma\theta_M$ be the standard deviation of the beam divergence introduced by the pulsed deflecting magnet.

Then, in order to pass three deviations in beam divergence in the deflecting system, the total divergence is $\sigma\theta_o \leq 1 \times 10^{-4}$, i.e.,

$$(\sigma\theta_o)^2 = (\sigma\theta_M)^2 + (\sigma\theta_1)^2 \leq 1 \times 10^{-4}$$

or

$$\sigma\theta_R \leq \left[(\sigma\theta_o)^2 - (\sigma\theta_1)^2\right]^{\frac{1}{2}}$$

Because $\frac{\theta_M}{\alpha} = \frac{\Delta B}{B}$ where $\alpha = 0.5^o$, then

$$\sigma\left(\frac{\Delta B}{B}\right) = \sigma\left(\frac{\theta_M}{\alpha}\right) = \frac{\sigma\theta_M}{\alpha}$$

This gives an rms error tolerance for $\Delta B/B$ of

$$\sigma\left(\frac{\Delta B}{B}\right) \leq \frac{\left[(\sigma\theta_o)^2 - (\sigma\theta_1)^2\right]^{\frac{1}{2}}}{\alpha}$$

If, for example, the beam divergence from the accelerator is $\sigma\theta_1 = 1 \times 10^{-5}$, then

$$\sigma\left(\frac{\Delta B}{B}\right) \approx 1.2 \times 10^{-2} \quad \text{or} \quad 1\% \text{ rms}$$

However, if $\sigma\theta_1 = 1 \times 10^{-4}$, $\sigma\theta_M$ should be zero.

Assuming a uniform intensity distribution for the electron beam from the machine, one obtains

$$\left|\frac{\Delta B_{max}}{B}\right| \leq \frac{1}{\alpha}\left[\left|\theta_o\right| - \left|\theta_1\right|\right]$$

Then, for example, using $\left|\theta_o\right| = 3 \times 10^{-4}$ and $\theta_1 = 3 \times 10^{-5}$, the result is

$$\left|\frac{\Delta B_{max}}{B}\right| \leq 3.2 \times 10^{-2}$$

One can estimate the beam divergence at the end of the accelerator using the results of the beam dynamics calculations. R. H. Helm and W.K.H. Panofsky* showed, from the integration of the radial equation of motion, that the accelerator waveguide structure is optically equivalent to a divergent lens with a focal length $F \approx 2L$, where L is the length of the accelerator. Then the angle of divergence at the end of the machine can be estimated from

$$\theta_1 \approx \frac{r_o}{F} = \frac{r_o}{2L} \leq \frac{1.15}{2 \times 3.3 \times 10^5} = 1.74 \times 10^{-6} \text{ radian}$$

where r_o is the maximum beam radius at the waveguide exit. Because the diameter of the waveguide iris is 2.23 cm, r_o should be less than 1.15 cm. This gives for θ_1, using 3.3 km for L, a divergence angle less than 1.74×10^{-6} radian.

---

*R.H. Helm and W.K.H. Panofsky, M-Report No. 201, Stanford Linear Accelerator Center, Stanford University, Stanford, California (November 1960).

Another way* to estimate the divergence angle θ_1 is to assume that there are no radial forces in the waveguide structure when the electrons are relativistic; this occurs a short distance (10 to 30 cm) after injection of the electrons into the machine. During acceleration the radial momentum (p_r) is constant, but the longitudinal momentum $p(z)$ increases linearly with distance,

$$p(z) = p_o + \epsilon z$$

where ϵ is typically 9 MeV/c per meter. The equation of the particle orbit in the waveguide structure can be written as

$$\frac{dr}{dz} = \frac{p_r}{p(z)} \quad , \quad p_r \ll p(z)$$

which can be integrated to

$$r(z) = r(0) + \frac{p_r}{\epsilon} \ell n \frac{p(z)}{p_o}$$

Using this equation, the divergence angle can be estimated as

$$\theta_1 \approx \frac{r(z) - r(0)}{L} = \frac{p_r}{\epsilon L} \ell n \frac{p(L)}{p_o}$$

The electrons will be injected into the accelerator at 80 keV energy; then using for the final momentum $p(L) = 20$ GeV/c, one obtains a divergence angle

$$\theta_1 \approx 10^{-5} \text{ radian}$$

and with this

$$\frac{\Delta B}{B} \approx 1\%$$

*H. DeStaebler, Jr., SLAC Report No. 9, Stanford Linear Accelerator Center, Stanford University, Stanford, California (November 1962).

This number, however, is an order of magnitude value only, because this calculation does not take into account the effect of possible asymmetries in the rf circuit for the acceleration waveguide, the possible radial electrical fields in the waveguide, and the misalignment of the whole accelerator. All these effects can increase the divergence angle of the electron beam.* Because of the statistical nature of these effects, an accurate beam divergence angle cannot be calculated. In order to minimize the beam divergence and the phase space introduced by the pulsed magnet system, the pulsed magnet modulators will be regulated so that

$$\sigma\left(\frac{\Delta B}{B}\right) \approx 1 \times 10^{-3}$$

or 0.1%.

*R. H. Helm and W.K.H. Panofsky, op. cit.

APPENDIX D

PHYSICAL PROPERTIES OF THE IGNITRON'S MERCURY PLASMA*

A. Gridless Tubes

First we consider the physical mechanism involved in the operation of a gridless ignitron with three electrodes (cathode pool, ignitor, and anode).

The ignitron conducts when current is passed through the ignitor into the mercury pool and the created charged particles, mostly electrons, ionize the mercury vapor between the cathode and anode regions. It was observed that the charge transport from the cathode to the anode in mercury discharge is invariably accompanied by high velocity jets of mercury vapor and the ejection of mercury droplets which travel at a velocity much slower than the accompanying pressure wave. The velocity of the vapor depends on the current density, but it is of the order of 10^5 to 10^6 cm/sec.

During the conduction cycle the mercury from the cathode pool is vaporized at a rate of approximately 7×10^{-3} grams per coulomb, and this mercury blast creates a pressure far in excess of the pressure as determined by the temperature. Therefore, under operating conditions it is possible for a pressure build-up to occur which will actually increase the product of the vapor pressure p and the gap between electrodes d, and with this cause a decrease in the maximum voltage value that the tube can hold off without breaking down (Paschen's law $E_{breakdown} \approx \frac{1}{pd}$).

The main loss mechanism for neutral particles from the cathode-anode region is the diffusion to the walls. This diffusion time constant can be calculated for simple tube geometrics; in the case of cylindrical volume with radius r_o and length ℓ (cathode-anode distance) it can be written as

$$\tau = \frac{1}{D}\left[\left(\frac{\pi}{\ell}\right)^2 + \left(\frac{2.405}{r_o}\right)^2\right]^{-1} = \frac{\Lambda^2}{D}$$

---

*J. L Cole and J. J. Muray, SLAC Report No. 31, Stanford Linear Accelerator Center, Stanford University, Stanford, California (July 1964).

noting that the diffusion coefficient of neutral gases changes with the pressure and temperature as

$$D(p,T) \approx D_o \left(\frac{T}{T_o}\right)^m \left(\frac{p_o}{p}\right)$$

where D_o is the value of D at $T_o = 273^\circ K$, $p_o = 760$ mm Hg, and $m \approx 1.5 - 1.75$.

With $D = 0.059$ cm^2/sec, $\ell \approx 10$ cm, and $r_o \approx 5$ cm, one obtains at $T = 38^\circ C$ and $T = 80^\circ C$,

$$\tau_{38^\circ} \approx \frac{p(mm)}{14.7} = 3 \times 10^{-4} \text{ sec} = 0.3 \text{ msec}$$

$$\tau_{80^\circ} \approx \frac{p(mm)}{14.7} = 6.8 \times 10^{-3} \text{ sec} = 6.8 \text{ msec}$$

The large value of τ clearly shows that at the elevated non-equilibrium pressure condition, a pressure build-up is possible when the repetition rate is higher than $1/\tau$, because the main loss mechanism is not sufficient to reduce the pressure between pulses. Thus, the maximum repetition rates at 38° and 80°, respectively, are

$$R_{max} \ (T = 38^\circ) = 3300 \text{ pps}$$

$$R_{max} \ (T = 80^\circ) = 147 \text{ pps}$$

This clearly shows the severe limitation in repetition rate of the ignitron switch tubes.

The most critical parameters influencing the rate of the forward breakdown are the repetition rate and the temperature of the tube.

The discharge in the ignitron tube lasts until the pulse forming network delivers energy through the load. The fact that a much smaller field than that necessary for breakdown is usually required to maintain the plasma suggests that the ionization efficiency is larger than during the tube breakdown. One possible mechanism that reduces the escape rate of

the electrons in the conduction cycle is a change from the free electron diffusion to an ambipolar diffusion. In this case the drift velocity of the plasma constituents is neither that of the ion nor that of the electron, but is determined by the ambipolar diffusion coefficient. The effective diffusion coefficient common to both electrons and ions can be written as

$$D_A = \frac{\mu^+ D^- - \mu^- D^+}{\mu^+ - \mu^-}$$

or, using the fact that the mobilities of the ion μ^+ and electron μ^- are related to the corresponding diffusion coefficients D^+ and D^-, one can write

$$D_A = \frac{D^+ D^- \left[(1/kT_+) + (1/kT_-)\right]}{(D^+/kT_+) + (D^-/kT_-)} \approx D^+\left(\frac{T_-}{T_+}\right)$$

because $T_- > T_+$ and $\frac{D^+}{kT_+} = \frac{\mu_+}{e} < \frac{\mu_-}{e} = \frac{D^-}{kT_-}$.

This ambipolar diffusion coefficient can be estimated as

$$D_A = D_+\left(\frac{p_o}{p}\right)\left(\frac{T_-}{T_+}\right) \approx \frac{D}{5}\left(\frac{p_o}{p}\right)\left(\frac{T_-}{T_+}\right)$$

$$D_A = 1 \times 10^{-2}\left(\frac{760}{p}\right)\left(\frac{T_-}{1500}\right)$$

where it is assumed that the ion temperature is of the order of $1500^{\circ}K$. With these values, where the electron temperature $T_- = 23{,}000^{\circ}K$, the diffusion time constant will be

$$\tau_{Diff} = \frac{5\Lambda^2}{D\left(\frac{T_-}{T_+}\right)} = \frac{\Lambda^2}{D_A}$$

and from this

$$\tau_{Diff} \approx 30 \text{ μsec at } 20^{\circ}C$$

$$\tau_{Diff} \approx 115 \text{ μsec at } 38^{\circ}C$$

$$\tau_{Diff} \approx 4000 \text{ μsec at } 80^{\circ}C$$

This time constant cannot be identified with the deionization time because other processes, such as the recombination and convection current to surfaces, can reduce the ion or electron density after the conduction cycle. The deionization time constant is actually composed of the decay constants of these processes in the form

$$\frac{1}{\tau_D} = \frac{1}{\tau_{Diff}} + \frac{1}{\tau_{conv}} + \frac{1}{\tau_R}$$

However, one can show that

$$\tau_{Diff} \approx \tau_{conv} \quad \text{and} \quad \tau_R \ll \tau_{Diff}, \tau_{conv}$$

It is known that at high repetition rates and high peak current operation the ignitron can break down in the reverse direction when reverse voltage is applied to the tube after the normal conduction cycle. The frequency of the arcbacks increases sharply with peak current and repetition rate at constant anode voltage.

The arcback can be defined as a failure of the voltage-holding capability of the tube in the reverse direction. This results in a flow of electron current in the reverse (anode to cathode) direction, due to the formation of a cathode spot on the anode.

It is believed by the authors that the primary cause of the arcback is the positive ion current flowing to the anode after the normal conduction cycle ends and the negative potential (reverse voltage) starts to build up on the anode.

In their classical paper, Kingdon and Lawton proposed that the arcbacks are due to the collection of positive ions on small insulating

patches on the anode. If the potential gradient exceeds the field emission limit of the anode material, electron emission can start from this "cathode spot" and this emission can result in arcback. The probability of spot formation naturally depends on the ion density after the conduction on the anode voltage, and on charge leakage from the insulating particles. Kingdon and Lawton state that the rate of arcback is proportional to the product of the initial inverse voltage (anode voltage) and the rate of the current (forward) change. This can be expressed in terms of an arcback factor δ as

$$\delta = V \frac{dI}{dt}$$

where

V = negative anode potential at the end of the forward conduction cycle in kilovolts

$\frac{dI}{dt}$ = rate of current change at the end of the forward conduction cycle in amperes per microsecond

This theory is proved by many experiments in ignitron rectifier service operation, but needs some extension to explain the significance of the Kingdon factor δ in modulator service. Quite generally, however, it may be said that in order to prevent the arcbacks, which are primarily caused by the back-streaming ion current to the negative anode, one should eliminate or at least minimize this ion current. The time dependence of this ion current is governed by the deionization processes, which are the space-charge limited flow from the plasma to the anode with a time constant of $\tau_{conv} \approx 30$ μsec, and the diffusion current to the walls with $\tau_D \approx 30$ to 100 μsec. These currents are proportional to the charge density ($n_+ \approx n_-$) in the plasma, and because n_+ and n_- depend on the forward current (mostly electron current $j_-/j_+ \approx 600$), one would expect the peak ion current to increase with the forward peak current. The typical values of plasma parameters for ignitrons tested in the modulator (WL5555, WL4681) are listed in Table I.

B. Gridded Ignitrons

The conventional gridded ignitron consists of a sealed envelope which contains a mercury pool cathode, ignitor electrodes, an anode, and one or more grids for various purposes. It is known that the operating temperature of a gridded ignitron is usually higher than for the gridless tubes. The reason for this is that the pressure is usually lower in the grid-anode region than between the cathode and the grid, and if the temperature is not high enough, current limitation can occur. A simple interpretation of the current limitation can be given based on the premise that the flux of positive ions to the tube walls cannot exceed the flux of neutral atoms into the grid-anode region. Despite the higher operating temperature and pressure, the gridded tubes can hold a higher voltage because they have much smaller spacings between the electrodes than do the gridless tubes.

The probability of the arcbacks is usually small or non-existent in the gridded tubes. The reason for this is that the back-streaming ion current to the anode is decreased due to the fact that the negative grid helps in the deionization process, and the total number of ions in the grid-anode region is smaller because of the small volume. The ion current to the negative grid shows the same type of time dependence that was reported here earlier flowing to the negative anode. The ion current decays with two different time constants which are, according to H. S. Butler and T. F. Turner,* 15.7 μsec and 35.6 μsec.

Generally then, gridded tubes can be used when operating conditions exceed the usual 60 pps operation or when the timing of the tube firing is extremely critical.

Two gridded tubes were tested in the pulse magnet modulator: the GE 5630, which was designed for high voltage operation, and the GE 7736, which was designed for ≈2.5 kV operation. Both tubes were operated with no observed breakdown at full voltage (5 kV) and current (160 amps).

---

*H. S. Butler and T. F. Turner, Proc. of the Symposium on Hydrogen Thyratrons and Modulators (May 1962).

TABLE I

PLASMA PARAMETERS FOR THE IGNITRONS TESTED

	20°C	38°C	80°C
Neutral Density n_o	3.8×10^{13} cm^{-3}	1.6×10^{14} cm^{-3}	
Ion, Electron Density $n_+ \approx n_e$	$\approx 2.4 \times 10^{12}$ cm^{-3}	$\approx 4.8 \times 10^{12}$ cm^{-3}	$\approx 1.3 \times 10^{13}$ cm^{-3}
(mm pd Hg × cm)	1.1×10^{-2}	5×10^{-2}	9×10^{-1}
Breakdown Voltage	> 50 kV	≈50 kV	≈3 kV
Neutral Diffusion Time Constant $\tau_o = \frac{\Lambda^2}{D_o}$		0.3 msec	6.8 msec
Neutral Mean Free Path		6.45×10^{-1} cm	2.82×10^{-2} cm
Thermalization Distance		< 6.45 cm	$< 2.82 \times 10^{-1}$ cm
Electron Temperature		23,000°K	10,000°K
Ambipolar Diffusion Time Constant $\tau_{Diff} = \frac{\Lambda^2}{D_A}$	30 μsec	115 μsec	4000 μsec
Time Constant for the Convection Ion Flow τ_{conv}		30 μsec	
Debye Thickness		10^{-3}	

LEGAL NOTICE